TECHNICAL MEMORANDUMS

NATIONAL ADVISORY COMMITTEE FOR AERONAUTICS

No. 736

# EFFECT OF FUSELAGE AND ENGINE NACELLES ON SOME AERODYNAMIC PROPERTIES OF AN AIRPLANE WING

By Joan Vladea

Zeitschrift für Flugtechnik und Motorluftschiffahrt
Vol. 24, No. 20, October 28, 1933



Washington
February 1934

NATIONAL ADVISORY COMMITTEE FOR AERONAUTICS

TECHNICAL MEMORANDUM NO. 736

# EFFECT OF FUSELAGE AND ENGINE NACELLES ON SOME AERODYNAMIC PROPERTIES OF AN AIRPLANE WING*

By Joan Vladea

With the aid of the method of J. Lotz (reference 1), the writer undertook to solve theoretically the lift distribution along the span of an airplane wing, when the outline of the wing is uneven. This problem arises in the case of a mid-wing monoplane with embedded engine nacelles. The fuselage and the nacelles were considered as aerodynamically profiled, that is, as lift-producing parts. The task was therefore to determine not only the disturbance caused by the fuselage and nacelles, but also their share in the total lift of the wing.

After the above-mentioned calculations, the induced velocity, due to the vortex system by which the wing was replaced, was also calculated and measured at the points corresponding, in an airplane, to the location of the horizontal tail surfaces. The tail was in fact wanting, so that its interference with the fuselage was disregarded. In order, however, to allow for the effect of this interference, use was made of some of the data published by Gorskyi (reference 2).

As mentioned by J. Lotz, the method discovered by her can also be used for wings in which discontinuities occur in the profile, angle of attack, or plan contour. The functions

$$f_1(\delta) = \alpha_{g(\delta)} \sin \delta = \Sigma \alpha_{g_n} \sin n \delta$$

$$f_2(\delta) = \frac{t_o}{t_{(\delta)}} \sin \delta = \Sigma \gamma_2 \cos 2 \delta$$

*"Über den Einfluss des Rumpfes (Gondeln) auf einige aerodynamische Eigenschaften des Flügels." Z.F.M., October 28, 1933, pp. 555-558.

fulfill the Dirichlet conditions which are necessary to develop a function in the Fourier series. In what follows, we undertake to determine the distribution of the lift and of the induced drag for the wing represented by figure 1. The profile for the wing is the Gottingen 723 and for the fuselage the Gottingen 360. These profiles have $c_l = 2.64$ and $c_l = 2.53$, respectively. The profile for the region of the nacelles was tested in the Aachen wind tunnel. It has $c_l = 2.64$, and the angle of attack for $c_a = 0$ is $-10.5^\circ$. If the assembly is also considered, the following differences between the angles of attack are obtained:

Wing-nacelles .... $-2^\circ$

Wing-fuselage .... $6^\circ$

For figure 1, we can write:

| Coordinates along wing | Angle of attack | Chord | $\left(\frac{dc_a}{d\alpha}\right)_{b\infty}$ |
|---|---|---|---|
| $0 < \delta < \delta_1$ | $\alpha_{(\delta)} = \alpha_1$ | $t_{(\delta)} = t_1$ | $c_l = c_{l1}$ |
| $\delta_1 < \delta < \delta_2$ | $= \alpha_2$ | $= t_2$ | $= c_{l2}$ |
| $\delta_2 < \delta < \delta_3$ | $= \alpha_1$ | $= t_1$ | $= c_{l1}$ |
| $\delta_3 < \delta < \pi - \delta_3$ | $= \alpha_3$ | $= t_0$ | $= c_{l3}$ |
| $\pi - \delta_3 < \delta < \pi - \delta_2$ | $= \alpha_1$ | $= t_1$ | $= c_{l1}$ |
| $\pi - \delta_2 < \delta < \pi - \delta_1$ | $= \alpha_2$ | $= t_2$ | $= c_{l2}$ |
| $\pi - \delta_1 < \delta < \pi$ | $= \alpha_1$ | $= t_1$ | $= c_{l1}$ |

The coefficients of the Fourier series are determined in the usual manner.

$$\alpha_{g_1} = \frac{2}{\pi}\int_0^{\pi} f_1(\delta)\,\sin\delta\,d\delta = \frac{2}{\pi}\left[\int_0^{\delta_1} \alpha_1 \sin^2\delta\,d\delta + \int_{\delta_1}^{\delta_2} \alpha_2 \sin^2\delta\,d\delta + \right.$$

$$+ \int_{\delta_2}^{\delta_3} \alpha_1 \sin^2\delta\,d\delta + \int_{\delta_3}^{\pi-\delta_3} \alpha_3 \sin^2\delta\,d\delta + \int_{\pi-\delta_3}^{\pi-\delta_2} \alpha_1 \sin^2\delta\,d\delta +$$

$$\left. + \int_{\pi-\delta_2}^{\pi-\delta_1} \alpha_2 \sin^2\delta\,d\delta + \int_{\pi-\delta_1}^{\pi} \alpha_1 \sin^2\delta\,d\delta\right] .$$

By integration we obtain:

$$\alpha_{g_1} = \frac{2}{\pi}(\alpha_1-\alpha_2)\left[(\delta_1-\delta_2) - \frac{1}{2}(\sin 2\delta_1 - \sin 2\delta_2)\right] + \frac{2}{\pi}(\alpha_1-\alpha_3)\left(\delta_3 - \frac{1}{2}\sin 2\delta_3\right).$$

We also obtain the coefficients $\alpha_{g_n}$ in the same way.

$$\alpha_{g_n} = \frac{4}{\pi}(\alpha_1 - \alpha_2)\left[\frac{\sin n\delta_1\cos\delta_1 - \sin n\delta_2\cos\delta_2 - n(\sin\delta_1\cos n\delta_1 - \sin\delta_2\cos n\delta_2)}{(n-1)(n+1)}\right] + \frac{4}{\pi}(\alpha_1-\alpha_3)\left[\frac{\sin n\delta_3\cos\delta_3 - n\sin\delta_3\cos n\delta_3}{(n-1)(n+1)}\right].$$

The amplitudes $\gamma_{2\nu}$ are determined by integrating between the same values as before.

$$\gamma_0 = \frac{1}{\pi}\int_0^{\pi} f_2(\delta)\,d\delta = \frac{2}{\pi}\left[\frac{t_0}{t_1} - \left(\frac{t_0}{t_1} - \frac{t_0}{t_2}\right)(\cos\delta_1 - \cos\delta_2) - \left(\frac{t_0}{t_1} - 1\right)\cos\delta_3\right].$$

$$\gamma_{2\nu} = \frac{4}{\pi}\left(\frac{t_0}{t_1} - \frac{t_0}{t_2}\right)\left[\frac{2\nu(\sin 2\nu\delta_1\sin\delta_1 - \sin 2\nu\delta_2\sin\delta_2) + \cos 2\nu\delta_1\cos\delta_1 - \cos 2\nu\delta_2\cos\delta_2}{(2\nu-1)(2\nu+1)}\right] + \frac{4}{\pi}\left(\frac{t_0}{t_1} - 1\right)\left[\frac{2\nu\sin 2\nu\delta_3\sin\delta_3 + \cos 2\nu\delta_3\cos\delta_3}{(2\nu-1)(2\nu+1)}\right] - \frac{4}{\pi}\frac{t_0}{t_1}\frac{1}{(2\nu-1)(2\nu+1)}\Bigg]$$

Since the calculation requires a constant $c_1$ over the whole wing span, this coefficient was determined as an arithmetical mean.

$$c_1 = c_{11} - (\cos\delta_1 - \cos\delta_2)(c_{11} - c_{12}) - (c_{11} - c_{13})\cos\delta_3.$$

The necessary coefficients for the equational system were calculated with the aid of these formulas, the unknowns being the coefficients $\alpha_{en}$ of the series

$$\Gamma(\delta) = V\,t_0\,c_1\,\Sigma\,\alpha_{en}\sin n\,\delta.$$

Since the convergence of the system was not very pronounced, eight harmonics were calculated.

For the case of a wing with only the fuselage, the solutions of the equational system are as follows:

$$\alpha_{e1} = 0.28821\ \alpha_1 + 0.03807\ \alpha_3$$

$$\alpha_{e3} = 0.04862\ \alpha_1 - 0.02483\ \alpha_3$$

$$\alpha_{e5} = -0.00083\ \alpha_1 + 0.01941\ \alpha_3$$

$$\alpha_{e7} = 0.00918\ \alpha_1 - 0.01526\ \alpha_3$$

$$\alpha_{e9} = -0.00476\ \alpha_1 + 0.01249\ \alpha_3$$

$$\alpha_{e11} = 0.00496\ \alpha_1 - 0.01019\ \alpha_3$$

$$\alpha_{e13} = -0.00360\ \alpha_1 + 0.00836\ \alpha_3$$

$$\alpha_{e15} = 0.00334\ \alpha_1 - 0.00717\ \alpha_3$$

With these values in the following points of the span

$$\delta = 15^\circ,\ 22\tfrac{1}{2}^\circ,\ 30^\circ,\ 45^\circ,\ 60^\circ,\ 67\tfrac{1}{2}^\circ,\ 75^\circ,\ 80^\circ,\ 90^\circ,$$

the values

$$\frac{t_o}{t_1}\ \alpha_{en} \sin n\ \delta$$

and

$$\frac{t_o}{t_1}\ \frac{n\ \alpha_{en} \sin n\ \delta}{\sin \delta}$$

were determined, which are proportional to the lift and to the induced velocity. The sums were multiplied by $t_o/t_1$, in order to obtain comparable data for fuselages of different lengths.

It is obvious that the coefficients $\alpha_{en}$ are functions of the angles of attack $\alpha_1$ and $\alpha_3$. Hence the distribution of the lift and of the induced velocity is also a function of the angle of attack. Figure 2 shows that the fuselage causes a disturbance in the distribution at small angles of attack, that this disturbance becomes zero at a certain angle of attack, and that, from there on, the fuselage share is greater than the disturbance produced by it. This

variation in the lift distribution is also accompanied by a variation in the induced drag, which is proportional to the deviation from the elliptical distribution. The function of the induced drag does not become zero when the function of the lift passes through zero. This interference effect can also be explained as follows. It is known that

$$d\,A = \rho\, V\, \Gamma\, d\,y = c_a\, \frac{\rho\, V^2}{2}\, t_{(\delta)}\, d\,y,$$

that is,

$$\Gamma = \frac{c_a}{2}\, V\, t_{(\delta)}.$$

The circulation is therefore proportional to $c_a\, t_{(\delta)}$. Figure 4 represents $c_a\, t$ as a function of $\alpha_e$ for the fuselage and wing. The straight lines intersect at a point where the interference is zero. The interference is proportional to the difference between $\alpha_e$ for the same value of $c_a\, t$.

From figure 2 it can then be seen that the lift does not become zero in the interval of the fuselage for zero angle of attack. Even in the interval of the fuselage the wing induces a lift which results in a positive angle of attack. This can happen only when there is an upward current in this region. This is also confirmed by the distribution of the induced velocity. Hence the induced drag becomes negative (thrust) in this region and at this angle of attack (fig. 5).

In the case of a wing with fuselage and engine nacelles the solutions of the equational system are:

$$\alpha_{e1} = 0.27817\,\alpha_1 + 0.01740\,\alpha_2 + 0.03840\,\alpha_3$$

$$\alpha_{e3} = 0.04904\,\alpha_1 - 0.00020\,\alpha_2 - 0.02480\,\alpha_3$$

$$\alpha_{e5} = 0.01525\,\alpha_1 - 0.01944\,\alpha_2 + 0.01913\,\alpha_3$$

$$\alpha_{e7} = -0.00204\,\alpha_1 + 0.01425\,\alpha_2 - 0.01472\,\alpha_3$$

$$\alpha_{e9} = -0.00013\,\alpha_1 - 0.00474\,\alpha_2 + 0.01237\,\alpha_3$$

$$\alpha_{e11} = 0.01345\,\alpha_1 - 0.01055\,\alpha_2 - 0.01035\,\alpha_3$$

$$\alpha_{e13} = -0.01019\,\alpha_1 + 0.00831\,\alpha_2 + 0.00846\,\alpha_3$$

$$\alpha_{e15} = 0.00291\,\alpha_1 + 0.00050\,\alpha_2 - 0.00716\,\alpha_3$$

Figure 6 shows that the influence of the nacelles is almost negligible, due to the unimpaired profile characteristics of the wing even in this region. The slightness of the influence is due to the angle of attack between this portion and the rest of the wing.

A comparison with practical results was made by means of wind-tunnel tests. The profile drag was added to the calculated induced drag. This drag was regarded, however, as proportional to the surface area of the model, which corresponds to the fact for normal angles of attack, since the frictional drag plays an important role at these angles (fig. 7).

As a practical result of the determination of the equation for the lift distribution, and hence also for the free vortices along the span of the wing, the induced vertical velocity in the elevator field was also calculated, both with and without the fuselage. A body of rotation with Gottingen profile 360 was used as the fuselage.

A few general formulas will now be established. The function $\Gamma = t_0 V c_1 \Sigma \alpha_{en} \sin n\delta$ will be used for the circulation distribution. The point A (fig. 8) is not situated on the axis of symmetry of the airplane, so that the required formulas have a general character. According to the Biot-Savart law, we can write:

$$d w_A = \frac{\Gamma l \, d y}{4\pi (l^2 + \xi^2)^{3/2}} + \frac{\frac{\partial \Gamma}{\partial y} d y}{4\pi} \left[ 1 + \frac{l}{(l^2 + \xi^2)^{1/2}} \right] =$$

$$= \frac{\Gamma d y}{4\pi l^2 \left[ 1 + \left( \frac{\xi}{l} \right)^2 \right]^{3/2}} + \frac{d\Gamma}{4\pi \xi} \left\{ 1 + \frac{1}{\left[ 1 + \left( \frac{\xi}{l} \right)^2 \right]^{1/2}} \right\}.$$

As customary, we put

$$y = -\frac{b}{2} \cos\delta \quad \text{and} \quad dy = \frac{b}{2} \sin\delta \, d\delta.$$

Then

$$\xi = d - \frac{b}{2} \cos\delta,$$

and

$$\frac{\xi}{l} = \frac{d}{l} - \frac{b}{2l} \cos\delta = \epsilon - \eta \cos\delta,$$

where $\epsilon = \frac{d}{l}$ and $\eta = \frac{b}{2l}$.

Substitution and integration yield

$$\frac{w_A}{V} = \frac{t_o c_1 b}{8 \pi l^2} \int_o^{\pi} \frac{\Sigma \alpha_{en} \sin n \delta \sin \delta}{\sqrt{[1 + (\epsilon - \eta \cos \delta)^2]^3}} d \delta$$

$$+ \frac{t_o c_1}{4 \pi l} \int_o^{\pi} \frac{\Sigma n \alpha_{en} \cos n \delta}{\epsilon - \eta \cos \delta} \left[ 1 + \frac{1}{\sqrt{1+(\epsilon-\eta \cos \delta)^2}} \right] d \delta .$$

Direct integration of the expressions is impossible, because the integrals are elliptical. It was therefore made graphically for the case when

$$\eta = 1 \quad \text{and} \quad \epsilon = 0.00;\ 0.05;\ 0.10;\ 0.15;\ 0.20;\ 0.25$$

and indeed for the wing without fuselage and for the wing with body-of-rotation fuselage. The accuracy of the drawing and of the planimetry was at least 0.001, so that the results compare very favorably with the results of a tedious analytical calculation.

For comparison with practical results, the angle was measured between the direction of motion at a point where the horizontal tail surfaces would be and a fixed initial direction. This angle was measured for the wing without fuselage and with the body of rotation. The initial direction was assumed to coincide with the direction of the wind at zero lift. For the wing with the Gottingen profile 723, with which these experiments were likewise performed, this zero lift was obtained at an angle of attack of $-6^{\circ}$. All the other angles were measured from this original direction.

The angles were measured with the aid of a very fine silk thread, as shown in figure 9. Silk was chosen because of its lightness and because its surface is rough enough for it to be blown in the direction of the wind. The angle, made by the silk thread with the initial direction, was measured with a telescope which was provided with a reticle and which could be rotated about its axis. The accuracy of this apparatus was $0.02^{\circ}$. In order to determine the effect of the weight of the thread, the angle of the thread was first measured in the customary suspen-

sion of the model in the wind tunnel and again after turning the model 180° about the axis AB. The angular difference thus obtained, which was about 0.3° at the same angle of attack, was used in the final determination of the angle. The angles were thus measured for the cases

$\eta = 1$ and $\epsilon = 0.00;\ 0.05;\ 0.10;\ 0.15;\ 0.20;\ 0.25.$

As shown by figures 10 and 11, the experimental results agree very well with the theoretical calculations for the case of a wing without fuselage. This proves that the assumptions were justified. There is no good agreement in the case of a wing with fuselage, due to the neglect of the lift distribution along the length of the fuselage in the theoretical calculations and to the failure to calculate sufficient harmonics. The assumption is justified that the whole lift can be concentrated in the center of pressure, on which assumption the calculation of the interference is based. For the case in question, the fuselage is much nearer to the test points than the wing or the center of pressure. Also the otherwise unimportant lift along the length of the fuselage has so much influence that this assumption is no longer justified. In the plotted curves, a great reduction in the induced velocity in the region covered by the fuselage can be detected, the induced velocity being even directed upward at small angles of attack. A considerable part of the region where these phenomena are noticeable is in the intervening space, where the influence of the tail surfaces is very weak (dead-air region). Therefore this disturbance phenomenon is not of very great importance. For the remaining region, the induced velocity measured has about the same value as for a wing without fuselage. Of course these values are also affected by the shape and width of the fuselage.

The following formula can be used in the case of a wing without fuselage for calculating the induced velocity along the span of the horizontal tail surfaces, since the induced velocity varies but slightly in this restricted region.

$$\frac{w_A}{V} \cong \frac{\eta^2}{2\pi\lambda} c_a \left(1 - \frac{3}{8}\eta^2 + \frac{15}{64}\eta^4 - \frac{175}{1024}\eta^6 + - \ldots\right) + \frac{2.3\, c_a}{\pi^2 \lambda}\left(1 + \frac{1}{\sqrt{1 + 0.7\,\eta^2}}\right).$$

The first part of the formula yields the induced velocity due to the supporting vortices; the second part, that due to the free vortices. For the case $\eta = 1$, the part due to the supporting vortices is about 1/3 of the total induced velocity and cannot therefore be disregarded. Of course this formula can be used only for fuselages of normal shape and width.

In the above-mentioned work of Gorskyi the shape of the curves for the vortices of the induced velocity are the same as in our case. He made the measurements with the aid of two pitot tubes under $90^{\circ}$, which were therefore also very sensitive for the direction of flow. He also measured the absolute value of the velocity at the points in question, which is not possible by our method. In general he obtained in the region covered by the fuselage a stronger upward current than we did. In the remaining region, the values are nearly the same. The interference between the tail surfaces and fuselage is not at all noticeable, the results being practically the same for both cases with and without tail surfaces. Gorskyi also measured the asymmetry in the downward current from the propeller.

I am indebted to Dr. C. Wieselsberger, the director of the aerodynamic institute, for the assignment of the subject, for his advice during the work and for the use of the wind tunnel for the control tests.

Translation by Dwight M. Miner,
National Advisory Committee
for Aeronautics.

## REFERENCES

1. Lotz, J.: Berechnung der Auftriebsverteilung beliebig geformter Flügel. Z.F.M., April 14, 1931, pp. 189-195.

2. Gorskyi, V. P.: Untersuchung über den Einfluss des Rumpfes und der Tragfläche auf horizontale Schwanzflachen des Flugzeuges," Moscow, 1932.

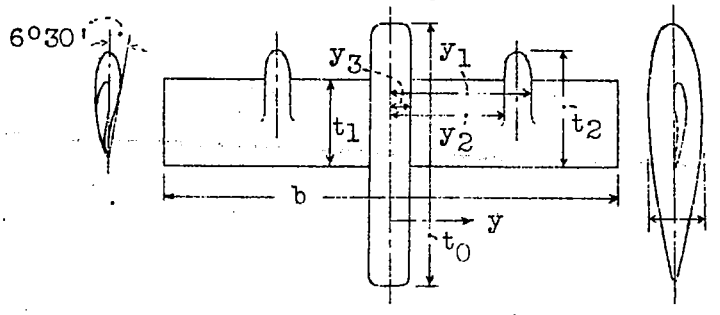


Figure 1.-Arrangement of fuselage and engine nacelles.

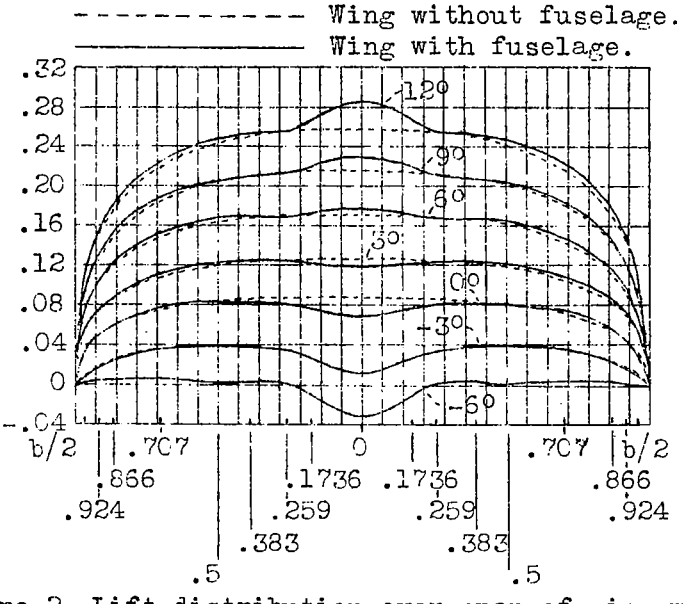


Figure 2.-Lift distribution over span of wing with fuselage.

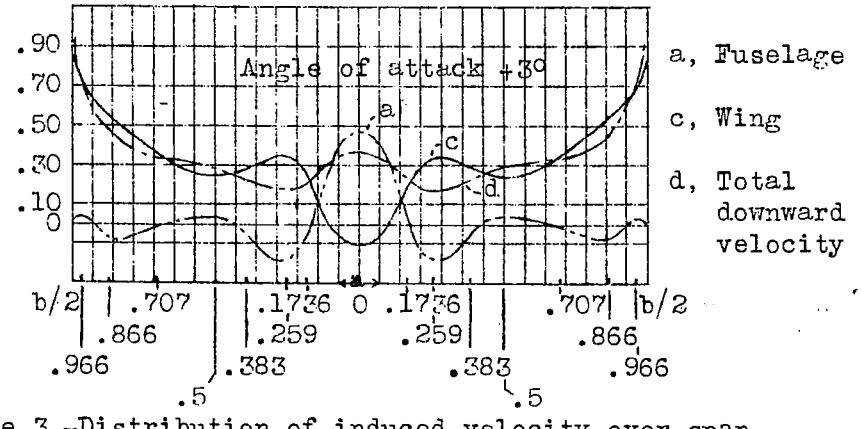


Figure 3.-Distribution of induced velocity over span of wing with fuselage.

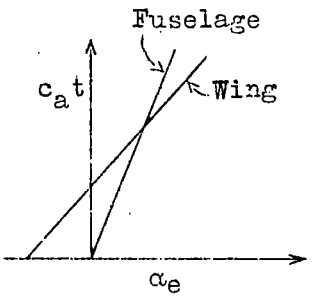


Figure 4.- Circulation for wing and fuselage plotted against angle of attack.

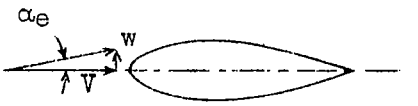


Figure 5.- Effective angle of attack induced on fuselage by wing at zero angle of attack.

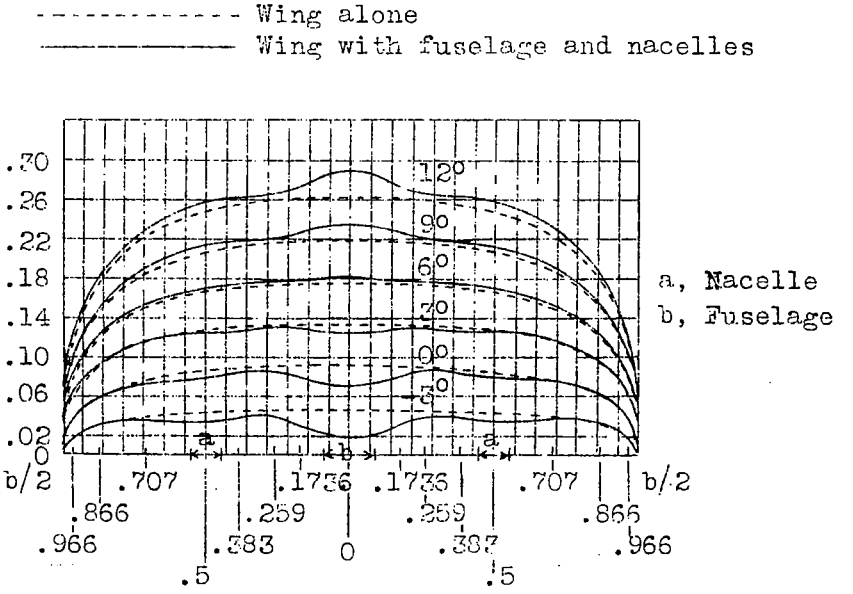


Figure 6.- Lift distribution over span of wing with fuselage and nacelles.

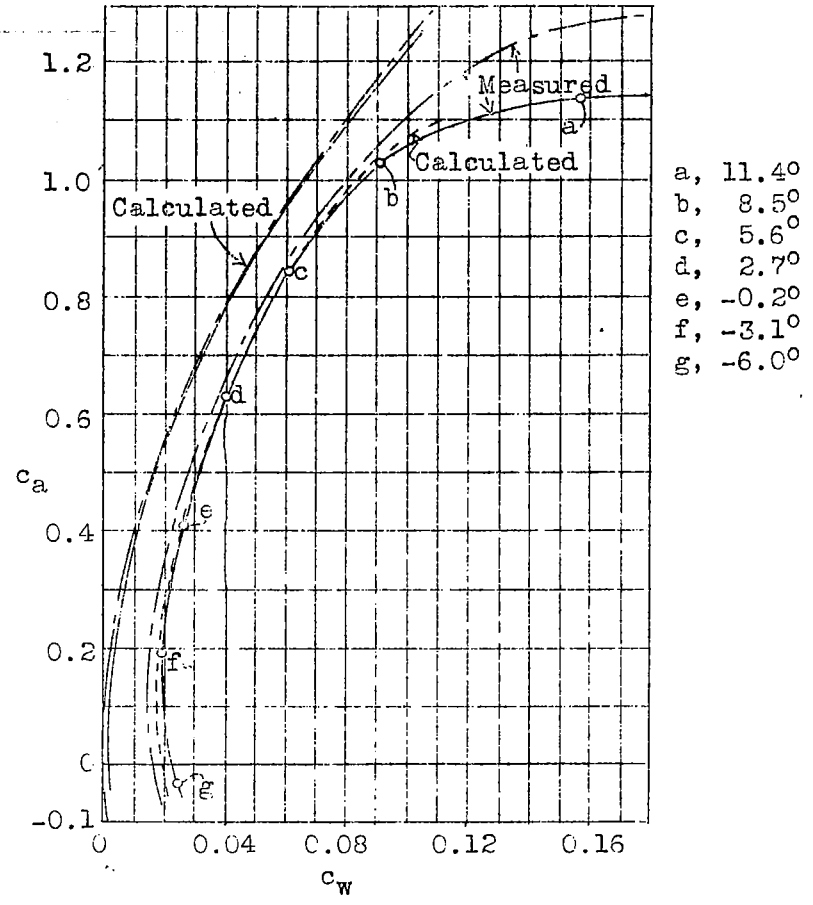


Figure 7.-Polars of wing alone and of wing with fuselage and nacelles calculated and measured.

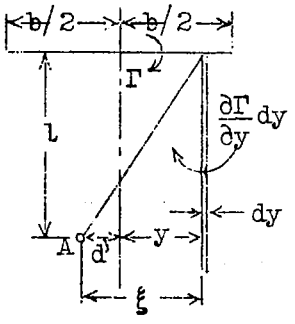


Figure 8.-For calculating downward current in region of horizontal tail surfaces.

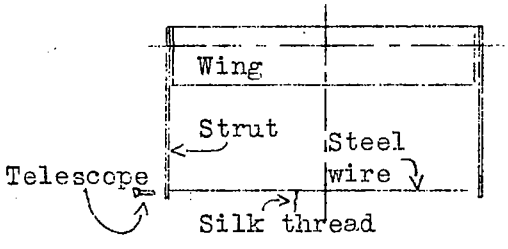


Figure 9.-Measurement of angle between direction of down current and wing chord.

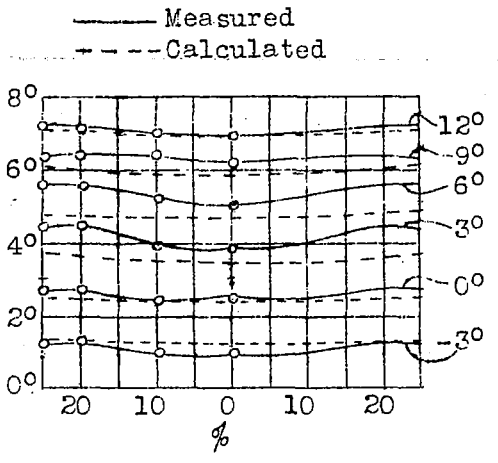


Wing without fuselage

Figure 10.-Direction of down current at horizontal tail surfaces vs. span(% of semispan)at various angles of attack of wing.

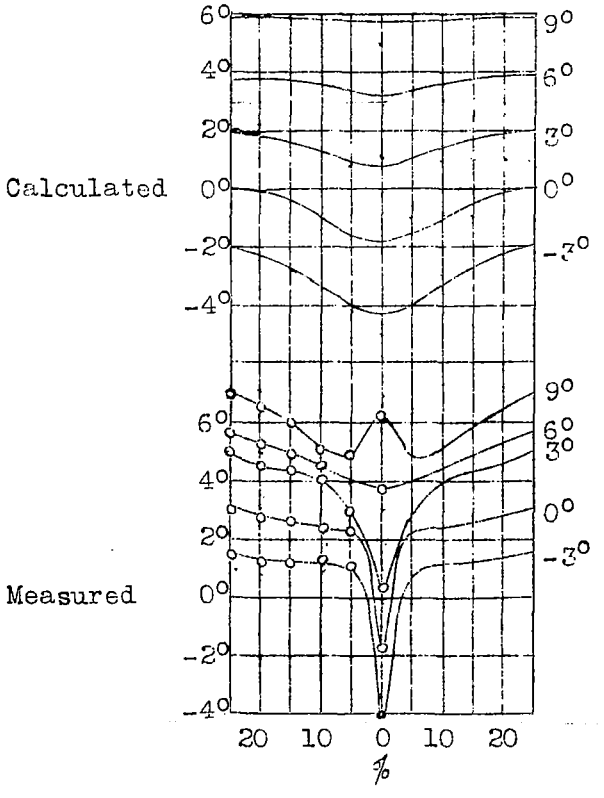


Wing with fuselage

Figure 11.-Direction of down current at horizontal tail surfaces vs. span(% of semispan) at various angles of attack of wing with fuselage.